Veterinary Microbiology 235 (2019) 151–163

Contents lists available at ScienceDirect

Veterinary Microbiology

journal homepage: www.elsevier.com/locate/vetmic

Cdc20 and molecular chaperone CCT2 and CCT5 are required for the Muscovy duck reovirus p10.8-induced cell cycle arrest and apoptosis

Quanxi Wang[a,1], Wei-Ru Huang[b,1], Wan-Yi Chih[b], Kuo-Pin Chuang[c], Ching-Dong Chang[d], Yijian Wu[a], Yifan Huang[a], Hung-Jen Liu[b,e,f,g,h,*]

[a] College of Animal Science, Fujian Agriculture and Forestry University, Fuzhou, Fujian 350002, China
[b] Institute of Molecular Biology, National Chung Hsing University, Taichung 402, Taiwan
[c] Graduate Institute of Animal Vaccine Technology, National Pingtung University of Science and Technology, Pingtung, 912, Taiwan
[d] Department of Veterinary medicine, National Pingtung University of Science and Technology, Pingtung, 912, Taiwan
[e] The iEGG and Animal Biotechnology Center, National Chung Hsing University, Taichung 402, Taiwan
[f] Rong Hsing Research Center for Translational Medicine, National Chung Hsing University, Taichung 402, Taiwan
[g] Ph. D Program in Translational Medicine, National Chung Hsing University, Taichung 402, Taiwan
[h] Department of Life Sciences, National Chung Hsing University, Taichung, Taiwan

ARTICLE INFO

Keywords:
Muscovy duck reovirus
p10.8
σC
p53
Fas
Apoptosis
Cell cycle arrest
Cdc20
CCT2
CCT5

ABSTRACT

This study demonstrates that the Muscovy duck reovirus (MDRV) p10.8 protein is one of many viral non-structural proteins that induces both cell cycle arrest and apoptosis. The p10.8 but not σC is a nuclear targeting protein that shuttles between the nucleus and the cytoplasm. Our results reveal that p10.8-induced apoptosis in cultured cells occurs by the nucleoporin Tpr/p53-dependent and Fas/caspase 8-mediated pathways. Furthermore, a compelling finding from this study is that the p10.8 and σC proteins of MDRV facilitate CDK2 and CDK4 degradation via the ubiquitin-proteasome pathway. We found that depletion of Cdc20 reversed the p10.8- and σC- mediated CDK4 degradation and p10.8-induced apoptosis, suggesting that Cdc20 plays a critical role in modulating p10.8-mediated cell cycle and apoptosis. Furthermore, we found that depletion of chaperonin-containing tailless complex polypeptide 1 (CCT) 2 and CCT5 reduced the level of Cdc20 and reversed the p10.8- and σC-mediated CDK4 degradation and p10.8-induced apoptosis, indicating that molecular chaperone CCT2 and CCT5 are required for stabilization of Ccd20 for mediating both cell cycle arrest and apoptosis. This study provides mechanistic insights into how p10.8 induces both cell cycle arrest and apoptosis.

1. Introduction

The p53 is well-known tumour suppressor protein and mediates DNA damage and apoptosis (Chen et al., 2009a, 2009b; Sperka et al., 2012). p53 is also the central regulator of cellular stress responses (Boyd et al., 2011). When cells are stressed by DNA damage, p53 becomes phosphorylated, which affects cell fate (Orth et al., 2012). p53 can be activated by sensor kinases, of which Ser15 and Ser20 are phosphorylated by ATM and Chk2, respectively (Maclaine and Hupp, 2009). Phosphorylation of p53 alleviates inhibition by MDM2 (Shieh et al., 1997). Modification of p53 enables the activation of its target genes involved in DNA repair, cell cycle arrest, and apoptosis (De Zio et al., 2013). Previous studies have suggested that nucleoporin Tpr plays a role in nuclear protein export (Frosst et al., 2002; Krull et al., 2004), regulating p53 nuclear-cytoplasmic trafficking (Funasaka et al., 2012; Huang et al., 2015).

Avian reovirus (ARV) is an important poultry pathogen which causes viral arthritis, chronic respiratory diseases, and malabsorption syndrome (Van der Heide et al., 1976; Heironymus et al., 1983). Muscovy duck reovirus (MDRV) is a highly pathogenic virus that causes epidemics of acute infectious disease in 4 to 45-day-old Muscovy ducklings (Wang et al., 2015a). In 2001, our group first confirmed that MDRV is the pathogen of Muscovy duck liver white-spot disease (Wu et al., 2001). Recent reports demonstrated that new types of MDRV cause hemorrhagic-necrotic lesions in the liver and spleen of sick birds and increase morbidity and mortality (Chen et al., 2009a, 2009b; Yuan et al., 2013; Yun et al., 2014). Therefore, it is important to elucidate the pathogenesis of MDRV and to propose efficient ways for prevention and control of MDRV infection. MDRV differs from ARV in the S1 and S4 genome segments and lacks the p17- and p10-encoding genes

* Corresponding author at: Institute of Molecular Biology, National Chung Hsing University, Taichung 402, Taiwan.
E-mail address: hjliu5257@nchu.edu.tw (H.-J. Liu).
[1] These authors contributed equally to this work.

https://doi.org/10.1016/j.vetmic.2019.06.017
Received 13 May 2019; Received in revised form 19 June 2019; Accepted 22 June 2019

(Schnitzer, 1985; Kuntz-Simon et al., 2002; Liu et al., 2003). Apart from the differences in coding assignment, clinical virulence is greater with MDRV than ARV.

Recently, our team demonstrated that the ARV p17 non-structural protein is able to suppress nucleoporin Tpr, leading to positively regulating p53, PTEN, and p21 and negatively regulating the PI3K/AKT/mTOR and ERK signaling pathways, both of which causes host translation shutoff and cell cycle arrest, induces autophagy, and benefits virus replication (Chi et al., 2013; Huang et al., 2015; Chiu et al., 2016, 2018). Apoptosis is one of the critical pathological mechanisms of reovirus infection (Salsman et al., 2005; Pruijssers et al., 2013). Pruijssers and colleagues suggested that apoptosis enhances reovirus replication in mouse brain, with consequent neurovirulence (Pruijssers et al., 2013). ARVs have also been demonstrated to induce cell death and tissue injury (Labrada et al., 2002; Shih et al., 2004; Lin et al., 2007, 2009b; Lin et al., 2011, 2015). The ARV σC protein induces apoptosis by modulating the DNA damage signaling, Src, p53, mitogen-activated protein kinase (MAPK), and protein kinase C delta (Lin et al., 2006, 2010, 2011). ARV-induced apoptosis elicits cytochrome c release from mitochondria to the cytosol (Chulu et al., 2007) and is associated with Bip/GRP79-mediated Bim translocation to the endoplasmic reticulum (Lin et al., 2015). The pathogenesis of ARV-induced apoptosis has been investigated in ARV-infected chicken tissues (Lin et al., 2007). Chickens infected with ARV caused tissue injury related to virus-induced apoptosis (Lin et al., 2007). Our previous study demonstrated that Muscovy duck reovirus (MDRV) causes histologic lesions in duck liver and spleen (Wu et al., 2001). In this work, MDRV-induced apoptosis in the duck liver and spleen was demonstrated. To date, the biological function of the MDRV p10.8 and σC proteins encoded by the MDRV S4 genome segment (Kuntz-Simon et al., 2002) remains largely unknown. Although we have shown previously that the MDRV p10.8 protein induces apoptosis and cell cycle arrest in cultured cells (Geng et al., 2009; Wang et al., 2018b, 2019), the precise mechanisms underlying MDRV p10.8-triggered apoptosis and cell cycle arrest and their regulation between apoptosis and cell cycle arrest remain largely unknown. This study further demonstrates that the MDRV p10.8 protein induces apoptosis in cultured cells via suppression of nucleoporin Tpr and activation of the p53 and Fas pathways. Another compelling finding presented in this study is that the MDRV p10.8 and σC proteins facilitate CDK4 and CDK2 degradation via the ubiquitin-proteasome pathway. Chaperonin-containing tailless complex polypeptide 1 (CCT), also known as tailless complex polypeptide 1 ring complex (TRiC), is a molecular chaperone found in the cytoplasm of all eukaryotes (Vallin and Grantham, 2019). The cell-division cycle protein 20 (Cdc 20) is an essential regulator of cell division that is encoded by the *CDC20* gene (Weinstein et al., 1994; Weinstein, 1997) in humans. Its most important function is to activate the anaphase promoting complex (APC/C) that initiates chromatid separation and entrance into anaphase. In the present study, we demonstrate that chaperonin-containing tailless complex polypeptide 1 (CCT) 2 and CCT5 are required for stabilization of Cdc20 and p10.8-induced apoptosis. We found that Cdc20 plays a critical role in mediating CDK4 degradation (Chen et al., 2019) and p10.8-induced apoptosis. This study has advanced our understanding on the mechanisms underlying MDRV p10.8-induced both cell cycle arrest and apoptosis.

2. Materials and methods

2.1. Virus and cells

The YB strain of MDRV was isolated and identified by our team (Wu et al., 2001). The virus was propagated in primary Muscovy duck embryo fibroblasts (MDEF). In this study, MDEF, immortalized chicken embryo fibroblast (DF-1), and Vero cells were grown in Dulbecco's modified Eagle medium (DMEM) containing streptomycin (50 μg/ml) and penicillin G50 (50 μg/ml), and supplemented with 10% fetal bovine serum (FBS) and 10 mM 4-(2-hydroxyethyl) piperazine-1-ethanesulphonic acid (HEPES) (pH 7. 2). Cells were seeded 1 day before each experiment in 6-cm cell culture dishes with 1×10^6 cells and grown at 37 °C in a 5% CO_2 humidified incubator. All cells were cultured in serum-free medium for 2 h followed by refreshing the medium containing 5% of fetal bovine serum (FBS) and continuing growth until cell confluence reached about 75%.

2.2. Reagents and antibodies

The Goscript™ Reverse Transcription System was from Promega Co. (Madison, USA). Annexin V-FITC was from Beyotime Biotechnology (Shanghai, China). MG132 was from Calbiochem Co. (San Diego, USA). Mouse anti-CDK2, mouse anti-CDK4 antibodies, mouse anti-GST, rabbit anti-nucleoporin Tpr, and mouse anti-ubiquitin antibodies were purchased from Santa Cruz Biotechnology (Dallas, USA). Rabbit anti-p-p53 (S15), mouse anti-p53, mouse anti-GST, rabbit anti-histone H2A, rabbit anti-CDC20 antibodies were from Cell Signaling (Danvers, USA). Rabbit anti-Fas, rabbit anti-Fas-associated death domain protein (FADD), mouse anti-cleaved caspase-8, and mouse anti-cleaved caspase-3 were purchased from Bioss (Beijing, China). Mouse anti-poly (ADP-ribose) polymerase (PARP) antibody was from BD Biosciences (Franklin Lakes, USA). Mouse anti-His, rabbit anti-CCT2, and rabbit anti-CCT5 antibodies were from Abcam (Cambridge, UK). Mouse anti-FLAG antibody was from Sigma-Aldrich Co. (St. Louis, USA). Mouse anti-β-actin antibody was from Millipore (Billerica, USA). Anti-mouse IgG (H + L) and anti-rabbit IgG (H + L) antibodies were purchased from Kirkegard & Perry Laboratories (Washington, USA).

2.3. Ethics statement

The animal protocol used in this study was approved by the Research Ethics Committee of College of Animal Science, Fujian Agriculture and Forestry University. All duck experimental procedures were carried out according to the Regulations for the Administration of Affairs Concerning Experimental Animals approved by the State Council of China.

2.4. Construction of the pCI-neo-flag-p10.8 and pCI-neo-flag-σC constructs

To study whether the MDRV p10.8 and σC proteins mediate cell cycle and apoptosis and to study whether the MDRV p10.8 and σC proteins interact with CDK4 or CDK2, both pCI-neo-flag-p10.8 and pCI-neo-flag-σC plasmids were constructed. The pCI-neo expression vector with an N-terminal flag sequence was constructed by our laboratory as previously described (Wu et al., 2017). Two pairs of degenerate primers were designed based on the p10.8- and σC-encoding genes of MDRV. The primers for amplifying the p10.8- and σC-encoding genes of MDRV are as follows: p10.8: forward 5′GGGAATTCAGCTGATGCTTTTGAAGT CCACT3′ and reverse 5′AGGCGGCCGCTTATTCATAGTTAGATCCCG AGA3′. σC: forward 5′AAGAA TTCATCCGAAACTCCCGCTCCTCCA3′ and reverse 5′AGCGGCCGCTATCAT AGTTAGATCCCGAGA3′. The underlines indicate the position of the restriction sites (Eco RI and Not I) in the primers. Viral RNA was extracted using the TIANamp Viral Total Nucleic Acid Purification Kit (Namp, Beijing, China) according to the manufacturer's instruction. Reverse transcription (RT) contained 3 μl of extracted RNA, 1 μl of primer (0.5 μg/μl), 2 μl of polymerase chain reaction (PCR) nucleotide mix (10 mM), 1 μl of GoScript™ reverse transcriptase, 4 μl of GoScript™ 5× reaction buffer, 2 μl of $MgCl_2$ (25 mM), 0.5 μl of recombinant RNasin ribonuclease inhibitor, and adjusted with nuclease-free water to a total volume of 20 μl. The reaction was carried out at 42 °C for 15 min and 72 °C for 15 min (Wang et al., 2015a). PCR was performed with 1 μl of cDNA, 0.5 μl of each primer, 1 μl of PCR mix, and 8 μl of ddH_2O, in a total volume of 20 μl. The PCR conditions for amplification were 95 °C for 5 min, 35 cycles of 95 °C for 30 s, 55 °C for 30 and 72 °C for 30 s (p10.8) or 1 min (σC), followed by 72 °C for 10 min. The products were electrophoresed on a 1% agarose gel. PCR

products were purified using an agarose gel DNA extraction kit (TIANamp). Purified PCR products were digested with *Eco*RI and *Not*I, followed by ligation into the same restriction sites of the pCI-neo-flag plasmid with T4 DNA ligase at 16 °C for 10 h. The recombinant plasmid was transformed into *E. coli* DH5α competent cells. Positive clones were selected by blue-white screening. Colonies containing positive clones were cultured at 37 °C for 12 h, and the recombinant plasmid was extracted and purified using a high purity plasmid extraction kit (TIANamp). The correctness of these constructs was assessed by DNA sequencing.

2.5. G0/G1 cell synchronization

To study the effect of the MDRV p10.8 and σC proteins on the regulation of cell cycle progression, Vero and DF-1 cells were synchronized as described previously (Chiu et al., 2018). Cells were G0/G1 phase synchronized using serum deprivation by maintenance of the cells in either DMEM containing no FBS supplementation for 72 h. Cells were transfected for 18 h with constructs (pCI-neo-flag, pCI-neo-flag-p10.8, and pCI-neo-flag-σC) after serum deprivation for 54 h. Cells were washed three times with PBS and fixed in PBS containing 70% ethanol at −20 °C. Cells were then treated with 50 μg/ml RNase and stained with 1 μg/ml propidium iodide for 30 min at 4 °C in the dark. The samples were immediately analyzed using a flow cytometer (FACSCanto II, BD). The percentage of cells in each phase of the cell cycle was analyzed by BD FACSDiva™ Software.

2.6. Histopathological examination by HE staining and flow cytometry analysis of MDRV-infected tissues

To investigate whether MDRV induces apoptosis in duck tissues, six 5-day-old specific pathogen France Muscovy duck were inoculated with the MDRV YB strain at an MOI of 2. France Muscovy ducks were purchased from Guangdong Wenshi Poultry Co. (China). Five days after infection, the sick ducks were slaughtered. RT-PCR was applied to detect MDRVs in liver and spleen tissues. The primer pair for amplification of the p10.8-encoding gene is as follows: forward, 5′-ATGGCTG ATG CTTTTGAAGT-3′ (1–20); reverse, 5′-TAGTTAGATCCCGAGAGC-3′ (271–288). The expected size of PCR products is 288 bp in length. The tissue samples were analyzed using a flow cytometer (FACSCanto II, BD). Histopathological lesions in the liver and spleen of France Muscovy ducks were examined by HE staining. Tissue sections were prepared as described previously (Wang et al., 2015b).

2.7. Isolation of the fractions of the cytosol and nucleus

To investigate the distribution of nucleoporin Tpr and p53 in the nucleus and the cytoplasm in p10.8-transfected Vero cells, the fractions of the cytosol and nucleus were isolated by using a CNM compartmental protein extraction kit according to manufacturer's protocol (BioChain Inc., Hayward, USA). The procedures were performed as described previously (Huang et al., 2015).

2.8. shRNA and siRNA

To explore the role of p53 in the regulation of apoptosis, Vero cells at 75% confluence were transfected with gene-specific shRNAs targeting p53, scrambled shRNA (29-mer non-effective scrambled pGFP-V-RS vector), and pGFP-V-RS vector, respectively. The p53 shRNA and scrambled shRNAs (TR30013) were obtained from OriGene Co. (Rockville, USA) and constructed in the vector pGFP-V-RS (TR30007). The p53 shRNA kit containing four different shRNA sequences, targeting the p53 gene, was tested in Vero cells. The one resulting in the most significant downregulation of p53 protein expression was chosen and used in this study as described previously (Huang et al., 2015). For Vero cells co-transfected pCI-neo-flag-p10.8 and p53 shRNAs, cells were transfected with the p53 shRNA plasmids for 6 h, followed by transfection with the pCI-neo-flag-p10.8 plasmid for 24 h. Whole cell lysates were collected for Western blot analysis. To explore whether the MDRV p10.8 protein induces apoptosis via the Fas signaling pathway, knockdown of Fas with the Fas siRNA was carried out. The Fas siRNA was purchased from Biomics Co. (Nantong, China). Vero cells transfected with a Fas siRNA for 6 h, followed by transfection with pCI-neo-flag (vector only) and pCI-neo-flag-p10.8 for 24 h post transfection. Whole cell lysates were collected for Western blot analysis.

To explore whether the role of Cdc20, CCT2, and CCT5 in the regulation of cell cycle and apoptosis, Vero cells at 75% confluence were transfected with gene-specific shRNAs targeting the Cdc20, CCT2, and CCT5 genes, respectively. Cdc20, CCT2 and CCT5 genes in the pLKO vector were obtained from the RNAi core facility (Academia Sinica, Taiwan). The shRNA sequences of Cdc20, CCT2, and CCT5 are as follows:

5′-AGACCAACCCATCACCTCAGT-3′ (accession number: NM_001255), 5′-TTATC GAGGAAGTCATGATTG-3′ (accession number:NM_006431), and 5′-GCTCCAAA GTGGTCAACAGTT-3′ (accession number: NM_012073), respectively. Vero cells transfected with the respective shRNA for 6 h, followed by transfection with pCI-neo-flag (vector only), pCI-neo-flag-p10.8 or pCI-neo-flag-σC for 24 h post transfection, respectively. Whole cell lysates were collected for Western blot analysis.

2.9. Co-immunoprecipitation assay

Experiments were initiated in serum-free medium for 2 h followed by refreshing the medium containing 5% of FBS overnight once cell confluency reached around 75%. To study whether the MDRV p10.8 and σC proteins interact with CDK2 or CDK4, co-immunoprecipitation assays were carried out as described previously (Huang et al., 2015). Immunoprecipitation was performed using the Catch and Release kit (Upstate Biotechnology) according to the manufacturer's protocol.

2.10. Protein expression and purification of Trx-His-p10.8 and GST-CDK2 fusion proteins

To construct pGEX4T-1-CDK2 plasmid, the CDK2 gene of Vero cells were amplified by RT-PCR using oligo dT and specific primer pairs (Forward: 5′GCG GAATTCATGGAGAACTTCCAAAAGGTGGAAAAG3′, 235–262; reverse: 5′AA ACTCGAGTCAAAGTCCAAGATGGGGTACT GGC'3, 1131-1110). The underline indicated the position of the restriction sites (*EcoRI and Xho I*) in the primers. The cDNA fragments representing the full-length CDK2 gene were generated by RT-PCR from total RNA of Vero cells. RT was performed using oligo dT primer as described above. PCR consisted of 2 μl of cDNA (500 ng), 2 μl of dNTP (2.5 mM), 1 μl of primer pairs, 0.5 μl of Pfu DNA polymerase (2.5 u), 5 μl of 10x Pfu buffer, and deionized water to a final volume of 50 μl. PCR amplification was performed under the following conditions: 95 °C for 5 min, 30 cycles of 95 °C for 1 min, 56 °C for 1 min, 72 °C for 1 min followed by a final 10 min extension at 72 °C. Purified PCR products were digested with the respective restriction enzymes and then introduced into the corresponding sites in pGEX4T-1 vector (GE Healthcare Life Sciences, UK). The recombinant plasmids were transformed into *E. coli* BL21 (DE3). The transformed *E. coli* were grown in Luria-Bertani (LB) broth with 100 ug/ml of ampicillin at 37 °C to an optical density of 0.6 and then induced with 0.4 mM of IPTG for 5 h at 28 °C. To further obtain soluble forms of GST-tagged fusion proteins, cells were collected by centrifugation followed by resuspension in lysis buffer [1x phosphate-buffered saline (PBS), 0.2 mM PMSF, 1% Triton X-100, 0.5% Sodium lauroyl sarcosinate]. After sonication, cell suspensions were centrifuged at 12, 000 x g for 20 min at 4 °C. Cell suspensions were changed to 1x PBS with Amicon Ultra 0.5-ml 10k filters (Millipore) by adding the same volume of 1x PBS at least five times. The cells were collected by centrifugation and resuspended in pGEX4T-1 system lysis buffer (1x PBS, 1% Triton X-100, 0.2 mM PMSF) and

sonicated. Cell suspensions were then centrifuged at 12,000 xg for 20 min at 4 °C. Each supernatant was applied to a glutathione-Sepharose 4B column (GE Healthcare Bio-Sciences). After washing beads with 1 x PBS washing buffer, the GST fusion proteins were eluted from the column with elution buffer (1x PBS, 10 mM reduced glutathione).

For construction of the pET32a -p10.8 plasmid, the p10.8-encoding gene of MDRV was amplified by RT-PCR using specific primers (Forward: 5′-GGGAATTC ATGGCTGATGCTTTTGAAGTCCACTAT-3′; reverse: 5′-AGGCGGCCGCTTATC TAGTTAGATCCCGAGA-3′). The underline indicated the position of the restriction sites (EcoRI and Not I) in the primers. Viral RNA was extracted using the TIANamp Viral Total Nucleic Acid Purification Kit (TIANamp) according to the manufacturer's instructions. Reverse transcription contained 3 μl of extracted RNA, 1 μl of primer (0.5 μg/μl), 2 μl of PCR nucleotide mix (10 mM), 1 μl of GoScript™ reverse transcriptase, 4 μl of GoScript™ 5× reaction buffer, 2 μl of $MgCl_2$ (25 mM), 0.5 μl of recombinant RNasin ribonuclease inhibitor, and adjusted with nuclease-free water to a final volume of 20 μl. The reaction was carried out at 42 °C for 15 min and 72 °C for 15 min (Wang et al., 2015a). PCR was performed with 1 μl of cDNA, 0.5 μl of each primer, 1 μl of PCR mix, and 8 μl of ddH_2O, in a total volume of 20 μl. The PCR conditions for amplification were 95 °C for 5 min; 35 cycles of 95 °C for 30 s, 55 °C for 30 s, and 72 °C for 30 s; followed by 72 °C for 10 min. The products were electrophoresed on a 1% agarose gel. PCR products were purified using an agarose gel DNA extraction kit (TIANamp). Purified PCR products were digested with *Eco*RI and *Not*I, followed by ligation into the corresponding sites of pET32a vector with T4DNA ligase at 16 °C for 10 h. The recombinant plasmid was transformed into *E. coli* DH5α competent cells. Positive clones were selected by blue-white screening. The recombinant plasmid pET32a-p10.8 was identified by DNA sequencing. Colonies containing positive clones were cultured at 37 °C for 12 h, and the recombinant plasmid was extracted and purified using a high purity plasmid extraction kit (TIANamp). The correctness of this construct was assessed by sequencing and by Western blot analysis with an anti-His antibody. The recombinant plasmid was then transformed into *E. coli* BL21 (DE3). The transformed *E. coli* cells were grown in Luria-Bertani (LB) broth with 100 mg/ml of ampicillin at 37 °C to an optical density of 0.6 and then induced with 0.4 mM of IPTG for 5 h at 28 °C. To purify His-tagged p10.8 fusion protein, cells were harvested by centrifugation, followed by resuspension in pET system lysis buffer (20 mM Tris-HCl pH 8.0, 300 mM NaCl, 0.2 mM PMSF, 10% glycerol, 5 mM imidazole) and sonicated. Cell suspensions were centrifuged at 12, 000 x g for 20 min at 4 °C. Each supernatant was applied to a nickel column. After washing beads with 150 ml washing buffer, His-tagged p10.8 fusion protein was eluted from the affinity column with elution buffer (20 mM Tris-HCl pH 8.0, 300 mM NaCl, 0.2 mM PMSF, 10% glycerol, 200 mM imidazole). Finally, His-tagged p10.8 fusion protein was changed to PBS buffer with Amicon Ultra 0.5-ml 10k filters (Millipore). Samples were stored at −20 °C until use.

2.11. GST pull-down assay

The procedures of GST pull-down assay were described previously (Chiu et al., 2018). Briefly, 1 ug of purified GST protein or GST-CDK2 was coupled to the glutathione-Sepharose 4B beads and incubated at 4 °C overnight with 100 ng of purified His-tagged p10.8 protein in binding buffer (20 mM Tris-HCl, 25 mM NaCl, 10% glycerol, 1 mM DTT, 1 mM EDTA, 1 mM PMSF, and 10 μg/ml cocktail protease inhibitor). The protein bound glutathione beads were then washed five times with binding buffer and eluted with elution buffer (50 mM Tris-HCl, pH 8.0, 10 mM reduced glutathione). Elution fractions were boiled and examined by Western blot assay.

2.12. RT-PCR was used to examine whether p10.8 and σC transcriptionally regulates CDk4 and CDK2

To investigate whether CDk4 and CDK2 transcription were downregulated by p10.8, σC or Cdc20, the CDk4 and CDK2 mRNA levels in pCI-neo-flag-p10.8 and pCI-neo-flag-σC transfected or Cdc20-depleted Vero cells were compared with those in mock treated cells. The primer pairs for amplification of the CDk4, CDK2, and GAPDH genes are as follows: CDK2 (EHH20842): forward: 5′-GGCCTAGCTTTCT GCCATT CTC-3′ (575–596); reverse, 5′-AAACTCGAGTCAAAGTCCAAGATGGG GTACTGGC-3′ (1131-1110). CDK4 (NM_001261347): forward, 5′-GAT TGGGCTG CCTCCAGAGG-3′ (862–881); reverse, 5′-TCTCAGTGTCCAG AAGGGAA- 3′ (1087-1068). GAPDH (NM_002046): forward, 5′-CACC ACCATGGAGAAGGCTG GGGCTCA-3′(480–506); reverse, 5′-GGCAGG TTTCTCCAGACGGCAGGTCAG-3′ (933-907).The expected sizes of PCR products of CDK2, CDK4, and GADPH are 557 bp, 226 bp, and 454 bp in length, respectively. In semi-quantitative RT-PCR amplification of the CDk4, CDK2, and GAPDH genes, Vero cells were transfected with pCI-neo-flag-p10.8 and pCI-neo-flag-σC plasmids for 24 h, respectively. The pCI-neo-flag-p10.8 and pCI-neo-flag-σC transfected cells were collected at 24 h postinfection (hpi). To investigate whether Cdc20 plays a critical role in mediating p10.8 and σC proteins of MDRV-mediated transcriptional downregulation of CDK4 and CDK2, Vero cells were transfected with a Cdc20 shRNA for 6 h, followed by transfection with pCI-neo-flag-p10.8 or pCI-neo-flag-σC plasmid DNA for 24 h. Total RNAs were extracted for semi-quantitative RT-PCR. After electrophoretic separation in an agarose gel, PCR products were stained with ethidium bromide.

2.13. Cell lysates preparation and Western blot assays

All tested cell lines from 6-well-dish plates were transfected with the pCI-neo-flag-p10.8- and pCI-neo-flag-σC plasmids for 24 h, respectively and collected and lysed in lysis buffer (50 mM Tris-HCl [pH 7.5], 150 mM NaCl, 1% Nonidet P-40, 0.5% sodium deoxycholate, and 0.1% sodium dodecyl sulfate (SDS) supplemented with complete protease inhibitor cocktail (Roche, Switzerland). 30 μg of total protein lysates from each treatment were quantified by a Bio-Rad protein assay (Bio-Rad Laboratories, USA), separated in a 12% SDS-polyacrylamide gel electrophoresis (PAGE) gel, and transferred to a PVDF membrane (GE Healthcare Life Sciences). Expression of each individual protein was examined using corresponding primary antibody and visualization by horseradish peroxidase (HRP) conjugated secondary antibody. After incubation with enhanced chemiluminescence (ECL plus) (Amersham/Pharmacia, Bucks, UK), the membrane was exposed to X-ray films (Kodak, Rochester, USA). The intensity of target proteins was calculated using Photocapt (Vilber Lourmat, France).

2.14. Statistical analysis

Data from the level of MDRV-induced apoptosis were evaluated for statistical significance and determined by Duncan's multiple range test (DMRT) by using SPSS

software (version 20.0). P values less than 0.05 were considered to be statistically significant.

3. Results

3.1. MDRV p10.8-induced apoptosis in MDEF cells and duck tissues

Our previous study demonstrated that MDRV induces apoptosis in DF-1 and Vero cell lines and causes histologic lesions in duck liver and spleen (Wu et al., 2001; Wang et al., 2018a, b; Wang et al., 2019). In this work, MDEF cells were infected with MDRV at multiplicity of infection (MOI) of 2 or transfected with the pCI-neo-flag-p10.8 or pCI-neo-flag-σC constructs for 24 h followed by flow cytometry analysis.

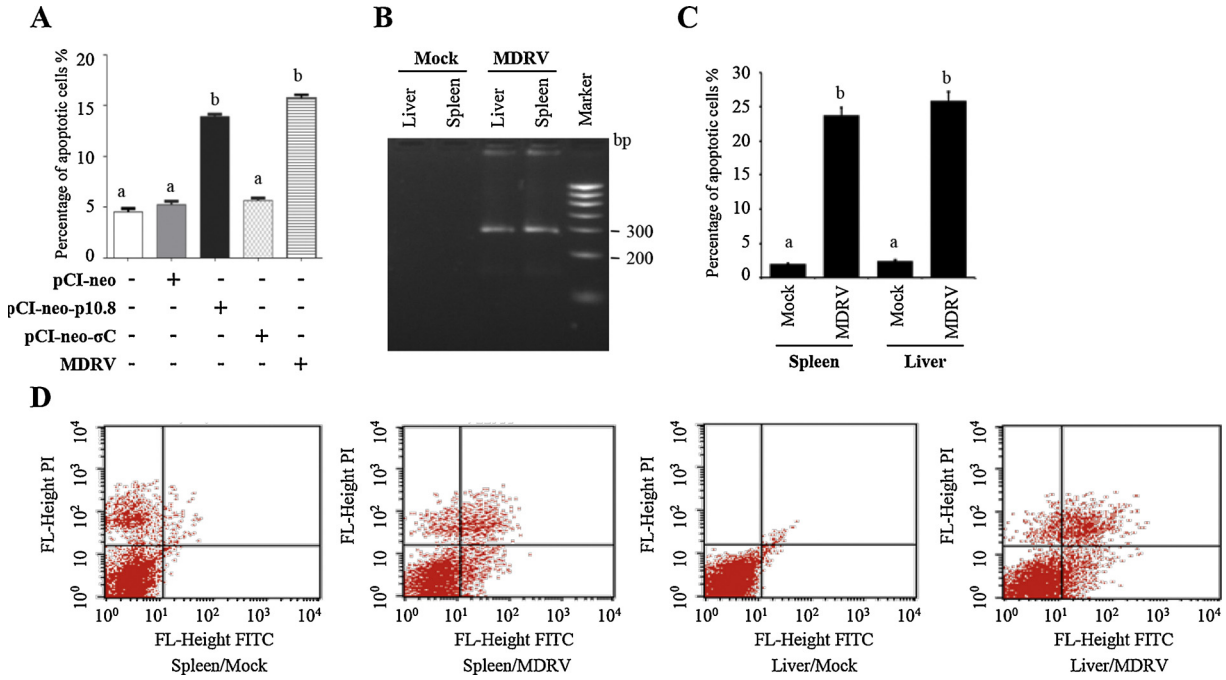

Fig. 1. MDRV induces apoptosis in MDEF cells and tissue cells. (A) MDEF cells infected with MDRV at an MOI of 2 were harvested at 24 h. Flow cytometry analysis of MDRV-infected cells as well as pCI-neo-flag-p10.8, and pCI-neo-flag-σC-transfected cells. After MDEF cells were infected MDRV and transfected with pCI-neo-flag-p10.8 or pCI-neo-flag-σC pCI-neo-p10.8 plasmids for 24 h, respectively, flow cytometry was used to detect the level of apoptosis. It is significantly higher than the mock-control cells and the pCI-neo plasmid-transfected cells. (B)To confirm MDRV in duck liver and spleen, RT-PCR was applied to amplify the p10.8-encoging gene of in MDRV-infected duck liver and spleen tissues. (C–D) Flow cytometry analysis of p10.8-induced apoptosis in MDRV-infected duck liver and spleen. Quantitation results were obtained. Apoptosis induction in MDRV-infected duck liver and spleen is significantly higher than the mock infected tissues, Significance between the treatments was determined by DMRT using SPSS software (Version 20.0). Means with common alphabets (a, b etc.) denote no significance at $P < 0.05$. Each value represents mean ± SE of three independent experiments.

MDRV-infected and pCI-neo-flag-p10.8-transfected MDEF cells are significantly higher than the mock-control cells (Fig. 1A). Having demonstrated that MDRV induces apoptosis in cultured cells, we next wanted to investigate whether MDRV induces apoptosis in liver and spleen. Histologic examination by HE staining of sick France Muscovy duck tissue sections reveals necrotic lesions in the liver and spleen, as report by Wu and colleagues (Wu et al., 2001). In this study, the p10.8-encoding gene of MDRV in duck tissues was examined by RT-PCR (Fig. 1B). Furthermore, MDRV-induced apoptosis in the duck liver and spleen was observed as revealed by flow cytometry analysis, but not mock-infected duck tissues (Fig.1C-1D). Apoptosis induction in MDRV-infected liver and spleen tissues is significantly higher than the mock infected ducks (Fig. 1C).Taken together, our results suggest MDRV-induced apoptosis in both cultured cells and duck tissues.

3.2. MDRV p10.8-induced apoptosis via suppression of nucleoporin Tpr and activation of p53

Although we have shown previously that MDRV p10.8-induced apoptosis through induction ER stress (Wang et al., 2018b, 2019), this study further investigated whether other pathways are involved in p10.8-induced apoptosis. Several reports have suggested that nucleoporin Tpr plays a role in nuclear protein export (Frosst et al., 2002; Krull et al., 2004) and regulates p53 nuclear-cytoplasmic trafficking (Funasaka et al., 2012; Huang et al., 2015). More recently, our team demonstrated that the ARV p17 protein functions as a nucleoporin Tpr suppressor that leads to p53 nuclear accumulation and consequently activates p53, p21, and PTEN (Huang et al., 2015). In this work, time course analysis of pCI-neo-p10.8- and pCI-neo-flag-σC-transfected Vero cells revealed that p10.8 was observed inside the nucleus 7 h post transfection and started to exit the nucleus14 h post transfection (Fig. 2A). The presence of σC protein in the nucleus was not observed (Fig. 2B). To rule out the possibility that nuclear p10.8 staining was an artifact of the immunofluorescence fixation conditions, its subcellular distribution was determined by an alternative approach. p10.8- and σC-transfected Vero cells were fractionated as indicated in the Material and Method, and the resulting cytoplasmic and nuclear extracts were examined by Western blot assays. The reliability of the fractionating method was evaluated by probing the blots with antibodies against Flag, β-tublin, and the nuclear protein histone H2A. Nuclear localization of p10.8 protein in Vero cells transfected with the pCI-neo-flag-p10.8 plasmid for 24 h was observed (Fig. 2A). As shown in Fig. 2B, σC protein was only detected in the cytoplasm. These data further confirm that the MDRV p10.8 protein localizes in the nucleus in agreement with a previous study (Guo et al., 2014). Since p10.8 localizes to the nucleus (Fig. 2A), we next wanted to examine the levels of p-p53 and nucleoporin Tpr in the nuclear extract. Our results reveal that increased levels of phosphorylated p53 were correlated with decreased levels of nucleoporin Tpr in p10.8-transfected cells, as revealed by Western blot assays (Fig. 2C–D), suggesting that nuclear import of p10.8 mediates activation of p53 probably via suppression of nucleoporin Tpr. Our finding is consistent with a recent report by Huang (Huang et al., 2015). No change was observed in σC-transfected cells (Fig. 2C). Interestingly, decreased levels of CDK4 and CDK2 were seen in p10.8- and σC-transfected cells (Fig. 2C).

Caspase 3 is a cysteine protease known to use PARP as a substrate *in vitro* (Los et al., 2002). Caspase 3 is produced as a proenzyme that has an apparent molecular size of 32 kDa and is activated as a result of its cleavage into two subunits, 12 KDa and 17 kDa, respectively (Lozano et al., 2009). PARP, a 116-kDa enzyme implicated in DNA single-strand damage repair, has been shown to be cleaved into two specific fragments (85 and 23 kDa) during the onset of apoptosis (Herceg and Wang, 2001). To further confirm that p10.8 induces apoptosis through the p53-dependent pathway, depletion of p53 was carried out. As shown in

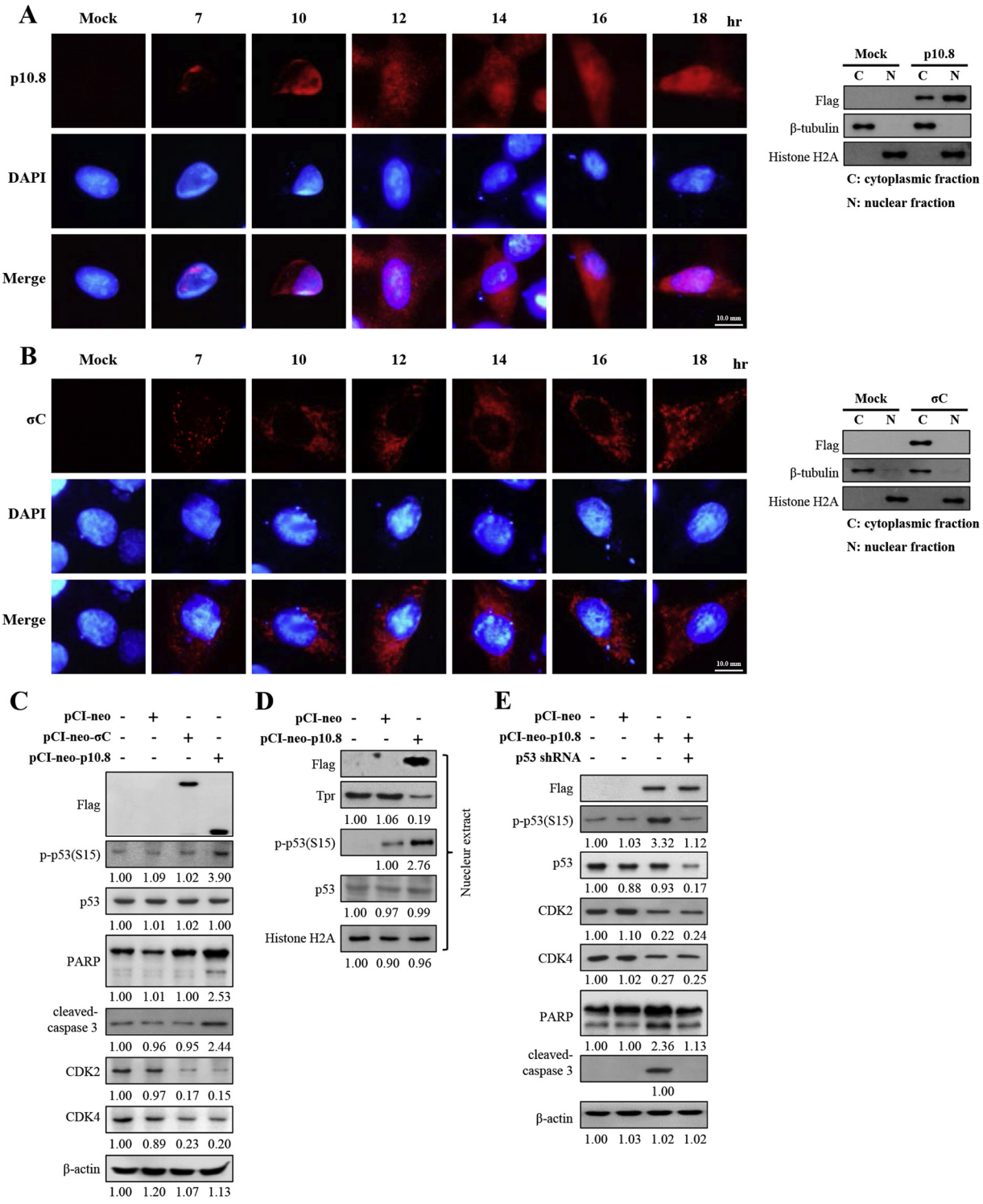

Fig. 2. The MDRV p10.8 protein localizes in the nucleus and induces the nucleoporin Tpr/p53 pathway to induce apoptosis. (A–B) Fluorescence microscopy analysis of intracellular distribution of the MDRV p10.8 (A) and σC (B) proteins at indicated time points was shown. Vero cells were transfected with pCI-neo-flag-p10.8 and pCI-neo-flag-σC plasmids, respectively. The cells were fixed with methanol and subsequently incubated with DAPI, with a mouse monoclonal antibody to flag. Western blot analysis of the cytoplasmic and nucleoplasmic fractions obtained from the transfected cells (right panels) with the indicated antibodies. (C) Upregulation of p53 and downregulation of nucleoporin Tpr by the MDRV p10.8 protein. To study whether p10.8 affects nucleoporin Tpr and p53, nuclear extracts from mock control (cells alone), pCI-neo-flag (vector only) and pCI-neo-flag-p10.8-transfected cells were collected at 24 h post transfection for Western blot assays. (D) To examine whether the MDRV p10.8 and σC proteins regulate p53, apoptosis and cell cycle, Vero cells transfected with mock control (cells alone), pCI-neo-flag (vector only), pCI-neo-flag-p10.8, and pCI-neo-flag-σC-transfected cells were collected at 24 h post transfection for Western blot analysis. The levels of p-p53, p53, cleaved PARP, cleaved caspase 3, CDK4, and CDK2 were examined. (E) To investigate whether the MDRV p10.8 protein regulates apoptosis via activation of p53, depletion of p53 with the p53 shRNA was carried out. Vero cells transfected with mock control (cells alone), pCI-neo-flag (vector only), pCI-neo-flag-p10.8, and pCI-neo-flag-p10.8/p53 shRNA were collected at 24 h post transfection for Western blot analysis. For cells co-transfected with pCI-neo-flag-p10.8 and p53 shRNA, Vero cells were transfected with the p53 shRNA plasmids for 12 h, and then transfected with the pCI-neo-flag-p10.8 plasmid for 24 h. Whole cell lysates were collected for Western blot analysis. Histone H2A was used as a loading control. The levels of p53 and cleaved PARP were examined. Either actin or histone H2A was used as loading controls. The activation and inactivation folds indicated below each lane were normalized against those at mock or vector alone.

Fig. 2E, the effect of p10.8 on the regulation of cleavage of caspase 3 and PARP was reversed partially in p53-knocked down cells, suggesting that p10.8 induces apoptosis at least in part through the p53 pathway. The finding is similar to the case of ARV σC-induced apoptosis (Shih et al., 2004; Chulu et al., 2007; Lin et al., 2009b). Interestingly, depletion of p53 did not reversed p10.8- or σC-mediated decreased levels of CDK4 and CDK2, indicating that p53 is not involved in regulation of CDK4 and CDK2 (Fig. 2E).

3.3. MDRV p10.8-induced apoptosis through the Fas/caspase 8 pathway

Having shown that MDRV p10.8 induces apoptosis via activation of p53, we next wanted to determine whether other upstream signaling and eff ;ector caspases are activated. Apoptosis can be activated via engagement of cell surface receptors such as the tumor necrosis factor alpha receptor and Fas (Luo et al., 1998; Lin et al., 2009a) which involves the FADD and subsequent activation of caspase 8 as well as release of cytochrome c from mitochondria into cytosol through the p53-dependent pathway (Kroemer et al., 1998; Chulu et al., 2007). In this work, increased levels of Fas, FADD, cleaved caspase 8, and cleaved caspase 3 in pCI-neo-flag-p10.8-transfected Vero cells were observed, as revealed by Western blot analysis (Fig. 3A). We detected significantly greater levels of cleaved caspase 8 and caspase 3 in p10.8-transfected cells as compared with mock infected cells 24 h post infection (Fig. 3A). Furthermore, the effect of p10.8-mediated apoptosis could be partially reversed by cells transfected with the Fas siRNA (Fig. 3B). Our results suggest that p10.8 induces apoptosis at least in part through the Fas/caspase 8 pathway. A model depicting MDRV p10.8-induced apoptosis through activation of the nucleoporin Tpr/p53 and Fas/caspase 8/caspase 3 pathways is shown in Fig. 3C.

3.4. p10.8 and σC proteins of MDRV mediate CDK4 and CDK2 degradation via the ubiquitin-proteasome pathway

As shown in Fig. 2C, p10.8 and σC proteins downregulate CDK4 and CDK2. We next wanted to explore the underlying mechanisms As shown in Fig. 4A, we demonstrate that a dramatic reduction in the CDK2 and CDK4 levels in pCI-neo-flag-p10.8- and pCI-neo-flag-σC-transfected Vero cells in a time-dependent manner. To investigate how MDRVp10.8 and σC down regulate CDK2 and CDK4, a proteasome inhibitor MG132 was used. In the presence of MG132, the levels of CDK2 or CDK4 in both p10.8- and σC-transfected cells could be reversed (Fig. 4B), suggesting that p10.8 and σC proteins facilitate CDK4 and CDK2 protein degradation via the ubiquitin-proteasome pathway. Since the levels of CDK4 and CDK2 in p10.8- or σC-transfected cells could be reversed in MG132-treated DF-1 cells, co-immunoprecipitation assays were carried out to examine the amounts of ubiquitin binding to CDK4 and CDK2. As shown in Fig. 4C–D, p10.8 and σC robustly enhanced ubiquitin targeting to CDK4 or CDK2, suggesting that the MDRV p10.8 and σC proteins mediate CDK4 and CDK2 degradation via the ubiquitin-proteasome pathway. Since the ARV p17 suppresses cell cycle CDKs and cyclins by direct binding to these proteins and by downregulating CDKs (Chiu et al., 2018), we also investigate whether p10.8 and σC suppress CDK4 and CDK2 by direct binding to CDK4 or CDK2. Co-immunoprecipitation assays were performed to test this hypothesis. Our results reveal that neither p10.8 nor σC interact with CDK2 or CDK4 (data not shown). To further confirm the result, an *in vitro* GST pull-down assay was carried out. Consistent with the results of co-immunoprecipitation assays, we found that these viral proteins do not interact with CDK2 (data not shown).

Having demonstrated that p10.8 and σC proteins of MDRV downregulate CDK4 and CDK2, we next wanted to study the phase in the cell cycle at which p10.8 and σC proteins inhibit cellular proliferation in Vero or DF-1 cells by flow cytometry. To assess the effect of these viral proteins on the regulation of cell cycle progression, the schematic flow

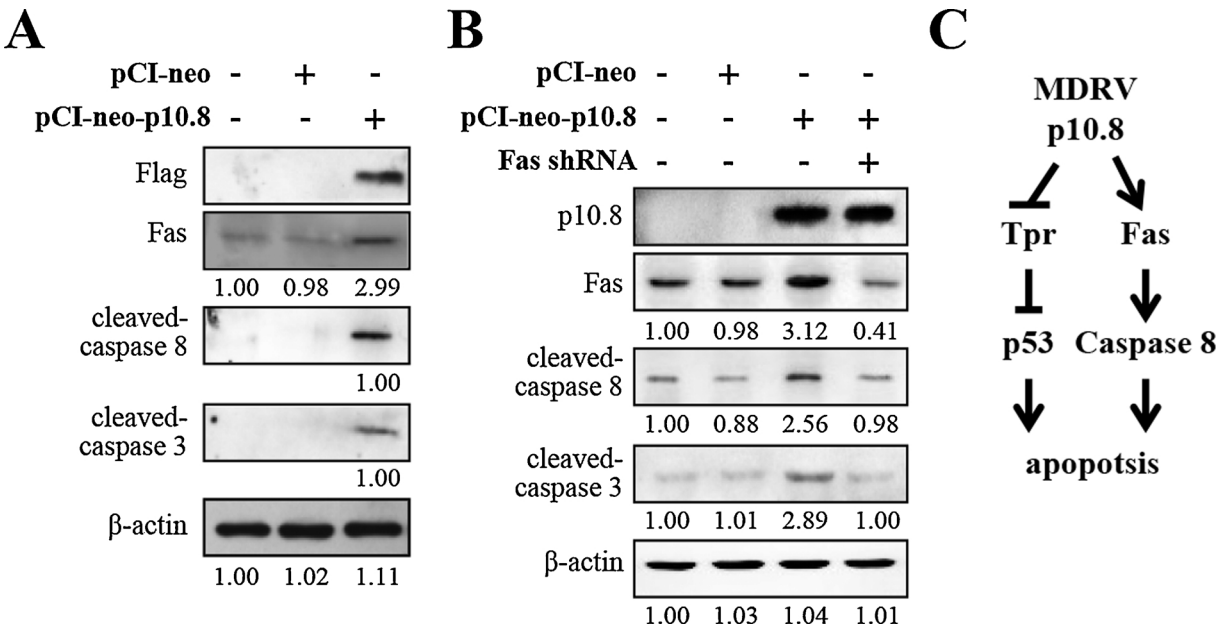

Fig. 3. MDRV p10.8-induced apoptosis mediated by the Fas pathway. (A) Vero cells were transfected with mock control (cells alone), pCI-neo-flag (Vector only) and pCI-neo-flag-p10.8 plasmids, respectively for 24 h. The expression levels of Fas, caspase-8 and cleaved caspase-3 were examined by Western blot assays. β-actin was used as a loading control. (B) To investigate whether the MDRV p10.8 protein induces apoptosis via the Fas pathway, depletion of Fas with the Fas siRNA was carried out. Vero cells transfected with mock control (cells alone), pCI-neo-flag (vector only), pCI-neo-flag-p10.8, and pCI-neo-flag-p10.8/Fas siRNA, respectively, were collected at 24 h post transfection for Western blot analysis. For cells co-transfected with the pCI-neo-flag-p10.8 and Fas siRNA, Vero cells were transfected with the Fas siRNA plasmids for 12 h, followed by transfection with the pCI-neo-flag-p10.8 plasmids for 24 h. Whole cell lysates were collected for Western blot assays. β-actin was used as a loading control. The levels of Fas, FADD, cleaved caspase 8, and cleaved caspase 3 were examined. (C) A model depicting that the MDRV p10.8 protein induces apoptosis via activation of the nucleoporin Tpr/p53 and Fas/caspase 8/caspase 3 pathways.

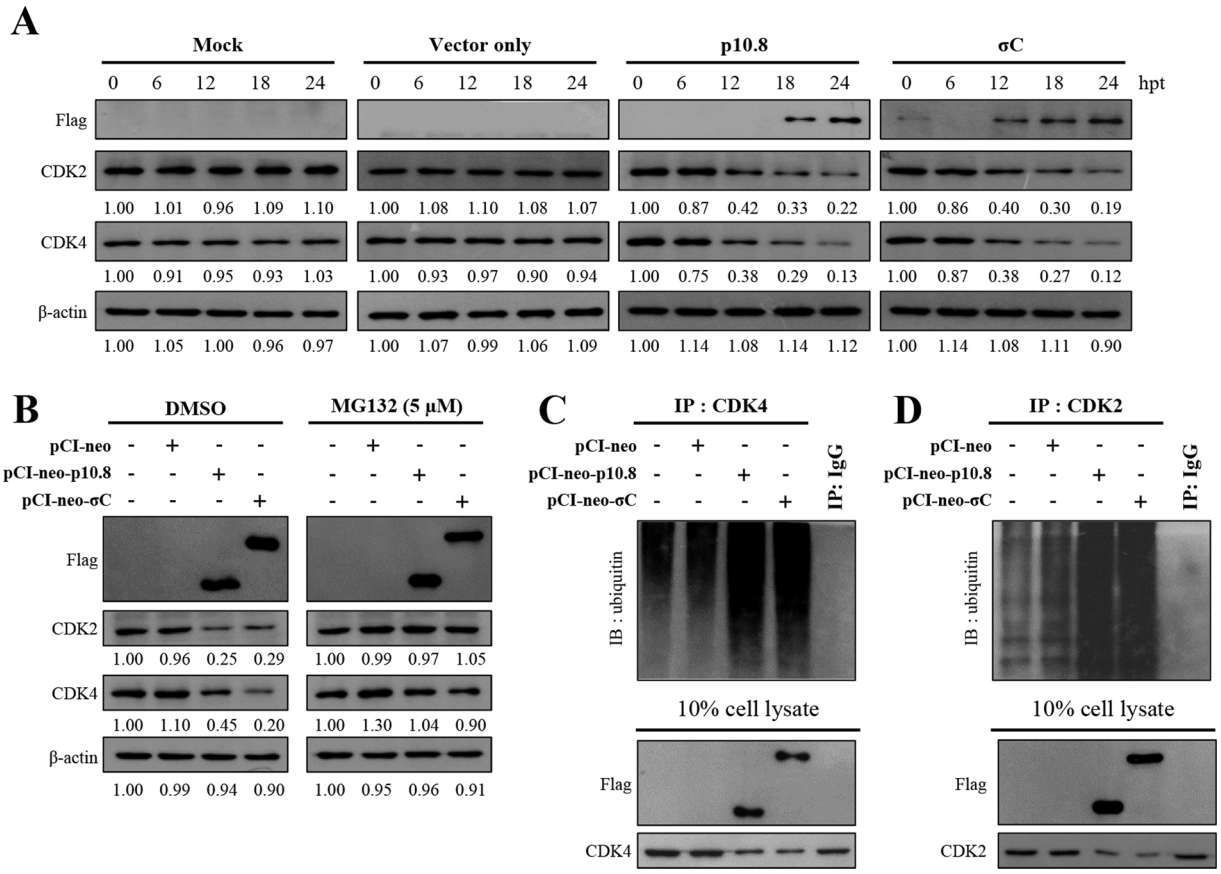

Fig. 4. p10.8 and σC proteins of MDRV mediate CDK2 and CDK4 degradation via the ubiquitin-proteasome pathway. (A) Levels of CDK2 and CDK4 in pCI-neo-flag-p10.8- and pCI-neo-flag-σC-transfected Vero cells were examined. Vero cells were collected at the indicated points, and whole cell lysates were harvested for Western blot analysis. Mock (cells alone) and mock-transfection (vector only) were used as negative controls. Signals in all western blots were quantified with Image J software. The levels of indicated proteins in the mock control (0 h) were considered one fold. The protein levels were normalised to those for β-actin. The activation fold indicated below each lane were normalized against values for the mock control (0 h). (B) The levels of CDK2 and CDK4 were examined in Vero cells without treatment (DMSO group) or pretreated with MG132, followed by mock transfection, pCI-neo-flag-p10.8, and pCI-neo-flag-σC transfection, respectively. The levels of indicated proteins in the mock control of untreated and treated groups were considered one fold. Protein levels were normalised to those for β-actin. The activation fold indicated below each lane were normalized against values for the mock control. (C–D) Co-immunoprecipitation assays examined the amounts of ubiquitin binding to CDK2 or CDK4 in pCI-neo-flag-p10.8- and pCI-neo-flag-σC-transfected cells. Rabbit IgG served as a negative control. Ten percent input of cell lysates served as loading controls.

chart shown in Fig. 5A depicts the steps of G0/G1 cell synchronization and sample collection. Vero cells require 15 h to complete a round of cell cycle while p10.8- and σC-transfected Vero cells need 24 h to complete the cell cycle (Fig. 5B). Our results reveal that both p10.8 and σC proteins result in cell cycle retardation (Fig. 5B) as compared to mock groups (cells alone and vector only). Representative cell cycle profiles of Vero cells transfected by p10.8 or σC are shown in Fig. 5B. A similar trend to Vero cells was seen in DF-1 cells.

3.5. Cdc20 plays a critical role in mediating p10.8 and σC proteins of MDRV-mediated CDK4 degradation

Having demonstrated that the p10.8 and σC proteins of MDRV facilitate CDK2 and CDK4 degradation via the ubiquitin-proteasome pathway, we next wanted to explore whether any host factor(s) regulate CDK4 and CDK2 degradation. We found that depletion of Cdc20 reversed the p10.8- and σC-mediated CDK4 degradation and p10.8-induced increased level of cleaved caspase 3 (Fig. 6A), suggesting that Cdc20 plays a critical role in mediating CDK4 degradation and p10.8-induced apoptosis. To examine whether CDk4 and CDK2 transcription were down-regulated by p10.8 or σC, the CDk4 and CDK2 mRNA levels in pCI-neo-flag-p10.8 and pCI-neo-flag-σC transfected were examined by RT-PCR. As shown in Fig. 6B, no change was observed in p10.8- or σC-transfected cells. Furthermore, mRNA levels of CDk4 and CDK2 in Cdc 20-depleted Vero cells were also not altered (Fig. 6B, lane 6). These results suggest that CDk4 and CDK2 are not transcriptionally down-regulated by p10.8, σC, or Cdc20.

To further confirm whether Cdc20 facilitates MDRV p10.8- and σC-mediated CDK4 degradation, co-immunoprecipitation assays were carried out. Our results reveal that increased amounts of ubiquitin binding to CDK4 or CDK2 in pCI-neo-flag-p10.8- and pCI-neo-flag-σC-transfected Vero cells were observed (Fig. 6C–D). Depletion of Cdc20 reversed the p10.8- and σC-mediated ubiquitin binding to CDK4, suggesting that Cdc20 plays a critical role in mediating CDK4 degradation, but not CDK2. A model depicting that Cdc20 regulates p10.8 and σC proteins of MDRV-mediated CDK4 degradation is shown in Fig. 6E.

3.6. Molecular chaperone CCT2 and CCT5 plays a critical role in stabilizing Cdc20

In this study, depletion of molecular chaperone CCT2 and CCT5 reduced the level of Cdc20 (Fig. 7A–B), indicating that CCT2 and CCT5 is required for stabilization of Ccd20. Furthermore, depletion of molecular chaperone CCT2 and CCT5 reversed p10.8- and σC-mediated CDK4 degradation and p10.8-induced apoptosis (Fig. 7A–B), indicating that molecular chaperone CCT2 and CCT5 stabilize Ccd20 for mediating p10.8- and σC-induced cell cycle arrest and p10.8-induced apoptosis. This study provides novel insights into how p10.8 induces both cell

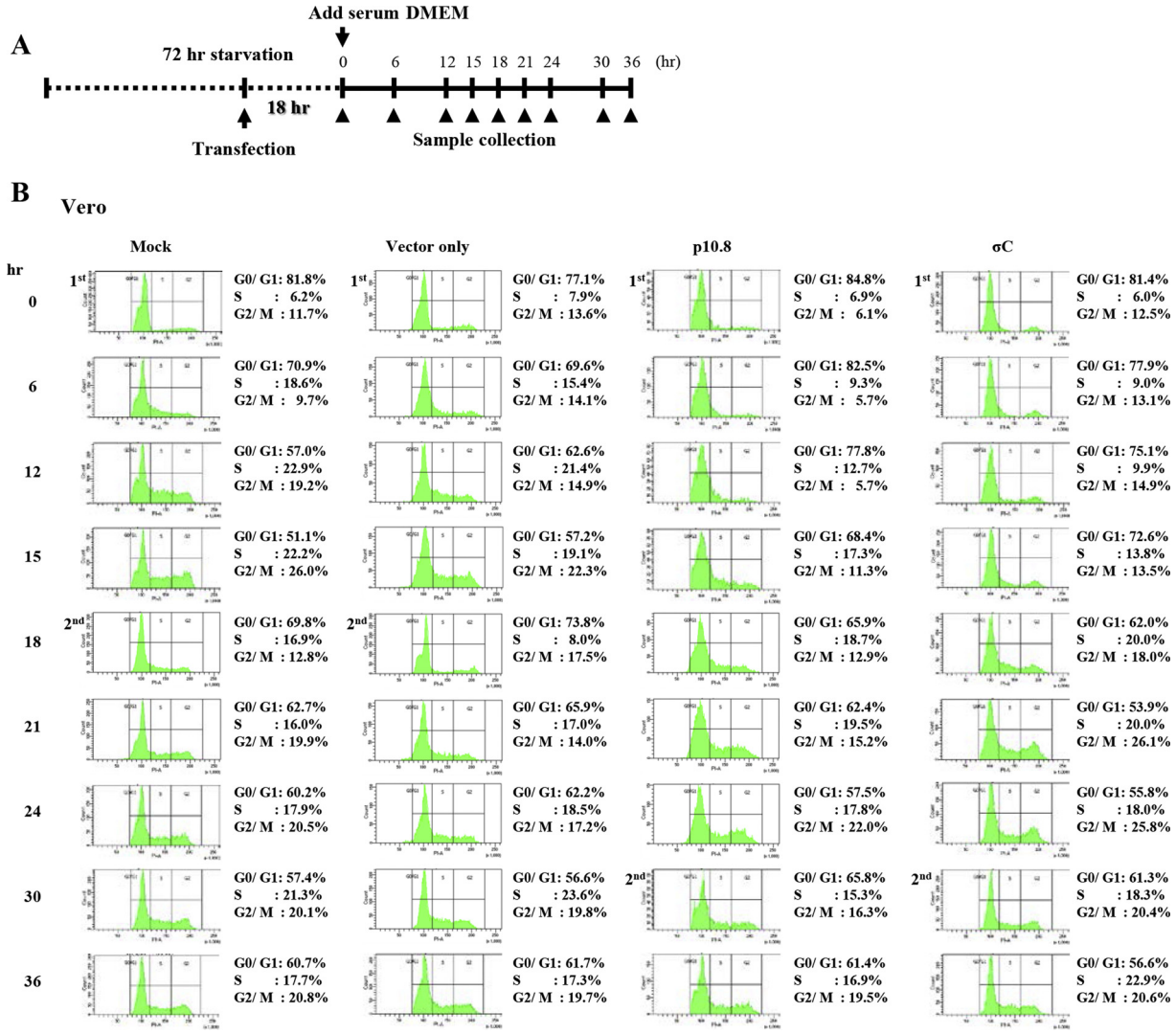

Fig. 5. Flow cytometry analysis of p10.8- and σC-mediated cell cycle retardation. (A) To assess the effect of these viral proteins on the regulation of cell cycle progression, the schematic flow chart depicts the steps of G0/G1 and G2/M cell synchronization and sample collection. (B) Representative cell cycle profiles of Vero cells transfected by p10.8 or σC are shown.

cycle arrest and apoptosis.

4. Discussion

The molecular mechanisms underlying MDRV-host interaction remain largely unknown and little information is available on the biological function of viral proteins. To explore the biological function of p10.8 and σC proteins encoded by the MDRV S4 genome segment, our team has undertaken a comprehensive study to investigate the roles of p10.8 and σC in mediating apoptosis and cell cycle. This study offers novel insights into how p10.8 and σC proteins mediate MDRV-induced apoptosis and G1/S cell cycle arrest. The MDRV p10.8 is a non-structural protein that differs from the ARV p10 protein in their biological function (Shmulevitz et al., 2004; Liu et al., 2008). Sequence analysis indicates that these non-structural proteins share low amino acid sequence identity. The ARV p10 is a membrane fusion protein, inducing cell-cell fusion (Shmulevitz et al., 2004; Liu et al., 2008) while our previous and current studies demonstrates that the MDRV p10.8 protein modulates apoptosis and G1/S cell cycle arrest (Wang et al., 2018b, 2019). Like the non-structural p17 protein of ARV (Costas et al., 2005), the non-structural p10.8 protein of MDRV is also a nuclear targeting protein and plays important roles in regulating virus-host interaction. Recent studies demonstrated a novel function for the ARV p17 protein whereby it acts as a Tpr suppressor and thus causing p53 and p21 nuclear accumulation and affecting cell cycle and host cellular translation (Liu et al., 2005; Huang et al., 2015; Chiu et al., 2016, 2018). This study identifies the MDRV p10.8 and σC proteins as new players in mediating CDK4 and CDK2 degradation via the ubiquitin-proteasome pathway, leading to cell cycle retardation.

Growing evidence shows that viral infection and viral protein expression causes cell cycle arrest to create a favorable environment for viral replication (Goh et al., 1998; Zhao and Elder, 2005; Li et al., 2009; Huang et al., 2015; Chiu et al., 2016, 2018). Thus, understanding of the molecular mechanisms underlying MDRV p10.8 and σC proteins-induced cell cycle arrest and apoptosis will provide insights into the biological significance of this effect during MDRV-host interactions. We show for the first time that the MDRV p10.8 protein targeting to the nucleus affects the nucleoporin Tpr/p53 pathway, leading to apoptosis. It was demonstrated that ARV p17-mediated cell cycle retardation in replication-activated cells allow the virus to access the host replication machinery without competing with cellular DNA replication, thereby enhancing virus replication (Chiu et al., 2016, 2018). Our recent study suggested that MDRV-induced apoptosis increases viral protein synthesis (Wang et al., 2019). Thus, the MDRV p10.8- and σC-induced cell cycle arrest to induce apoptosis may benefit virus replication. Apoptosis plays an important role in pathogenesis of many viral infections.

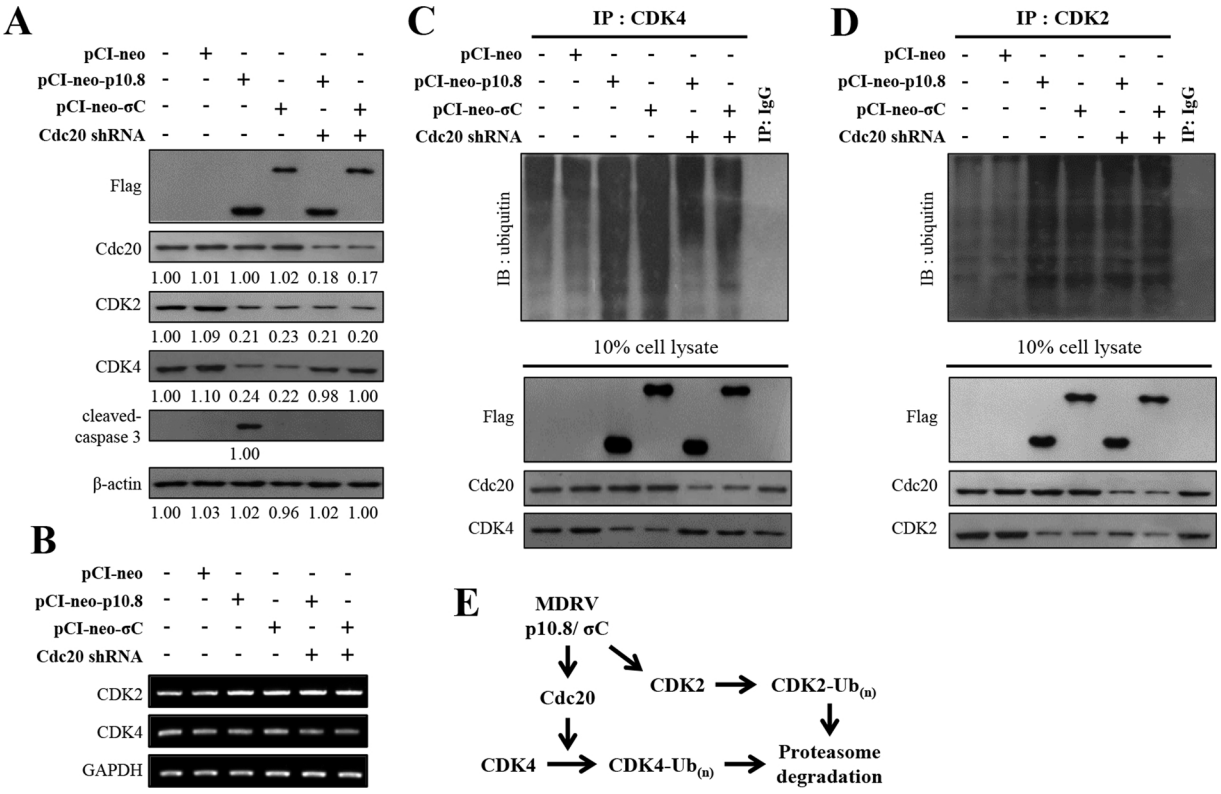

Fig. 6. Cdc20 plays a critical role in mediating p10.8 and σC proteins of MDRV-mediated CDK4 degradation. (A) To explore whether Cdc20 plays a critical role in mediating p10.8 and σC proteins of MDRV-mediated downregulation of CDK4 and CDK2, Vero cells were transfected with a Cdc 20 shRNA for 6 h, followed by transfection with pCI-neo-flag-p10.8 or pCI-neo-flag-σC plasmid DNA for 24 h. Levels of Cdc20, CDK4, CDK2, and cleaved caspase 3 in pCI-neo-flag-p10.8 or pCI-neo-flag-σC-transfected cells were examined. Signals in all Western blots were quantified with Image J software. The levels of indicated proteins in the mock control were considered one fold. The protein levels were normalised to those for β-actin. The activation fold indicated below each lane were normalized against values for the mock control. (B) To examine whether Cdc20 downregulates the CDK4 and CDK2 transcription in pCI-neo-flag-p10.8- or pCI-neo-flag-σC-transfected Vero cells, mRNA levels of CDK4 and CDK2 analyzed and compared with those in mock treated cells. In semi-quantitative RT-PCR, total RNAs were extracted for semi-quantitative RT-PCR. After electrophoretic separation in an agarose gel, PCR products were stained with ethidium bromide. (C–D) Co-immunoprecipitation assays examined the amount of the amounts of ubiquitin binding to CDK2 or CDK4 in pCI-neo-flag-p10.8- and pCI-neo-flag-σC-transfected cells. Vero cells were transfected with a.

Cdc20 shRNA for 6 h, followed by transfection with pCI-neo-flag-p10.8 or pCI-neo-flag-σC plasmid DNA for 24 h. Rabbit IgG served as a negative control. Ten percent input of cell lysates served as loading controls. (E) A model depicting that Cdc20 mediates p10.8 and σC proteins of MDRV-mediated CDK4 degradation.

Understanding the molecular basis for MDRV-host interaction and for MDRV-induced apoptosis can shed light on normal cellular events and on the specific ways that MDRV gains control over its hosts. Several viruses initiate apoptosis via both receptor and mitochondria-mediated caspase-dependent pathways (Kominsky et al., 2002; Chipuk and Green, 2005; Lin et al., 2009a). Our previous study has shown that the MDRV p10.8 induces endoplasmic reticulum stress to induce cell cycle arrest and apoptosis, benefiting viral protein synthesis (Wang et al., 2018b, 2019). This study further demonstrates that apoptosis induction by the MDRV p10.8 protein requires both the nucleoporin Tpr/p53 and Fas/caspase 8 pathways. Our findings suggest that MDRV induces apoptosis through caspase-mediated pathway, including activation of caspases 8 and 3 and cleavage of PARP.

The significance of apoptosis in the pathogenesis of mammalian reovirus (MRV)-induced tissue injure have been documented (Clarke and Tyler, 2003; O'Donnell et al., 2005; Lin et al., 2007; Clarke et al., 2009). MRV-induced cell death has been directly associated with myocarditis and lethal encephalitis in infected mice (Clarke and Tyler, 2003; O'Donnell et al., 2005; Clarke et al., 2009). In addition to inducing apoptosis in a variety of cell lines (Labrada et al., 2002; Shih et al., 2004), ARV-induced cell death was also detected in chicken tissues (Lin et al., 2007). It is of great importance to elucidate the pathogenesis of MDRV-induced apoptosis and to propose efficient ways for prevention and control of MDRV infection. Our results reveal that MDRV causes necrotic lesions (Wang et al., 2001) and induces apoptosis in the liver and spleen of MDRV-infected ducks. These findings suggest that a correlation between apoptosis and virus replication and tissue injure. This notion can be supported by previous studies (Chulu et al., 2007; Lin et al., 2007). More recently, Rodríguez-Grille and colleagues demonstrated that ARV-induced apoptosis could enhance both virus spreading and the processing of the viral non-structural muNS protein (Rodriguez-Grille et al., 2014).

This study provides evidence demonstrating that the MDRV p10.8 protein is one of many viral non-structural proteins, inducing both cell cycle arrest and apoptosis. A numbers of viruses, including MRV σ1s, human immunodeficiency virus (HIV) Vpr, and adenovirus E4orf4 proteins (He et al., 1995; Lavoie et al., 1998; Marcellus et al., 1998; Boehme et al., 2013; Murakami and Aida, 2014) cause both effects, whereas other viral non-structural proteins, such as influenza virus PB1-F2, Bunyaviral NSs protein (Colón-Ramos et al., 2003; Zamarin et al., 2005), ARV sigma C protein (Shih et al., 2004; Lin et al., 2006, 2010), ARV p17 protein (Chiu et al., 2018) directly induce either apoptosis or cell cycle arrest. Although our results indicate that p10.8 protein mediates both cell cycle arrest and apoptosis, it is not known how these effects are functionally associated until this work. Many viruses have been demonstrated to trigger cellular pathways that are activated by DNA damage or replication stress (Lin et al., 2011; Chaurushiya and Weitzman, 2009; Baer et al., 2012; Turnell and Grand, 2012) while other viruses use different strategies to cause cell cycle arrest and apoptosis by suppressing the activities of cell cycle control

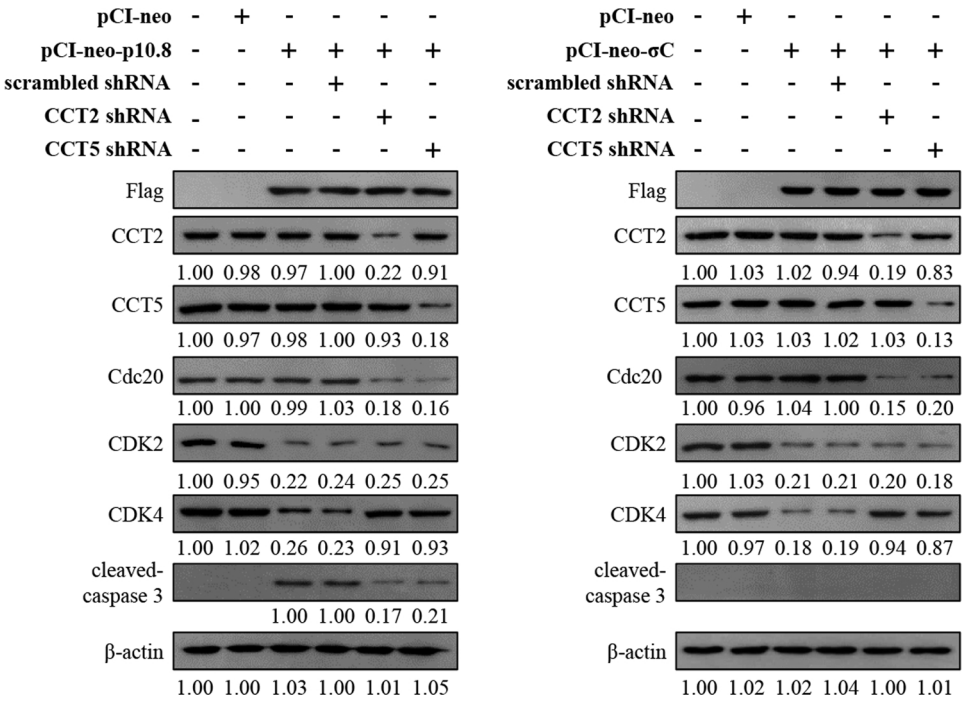

Fig. 7. Molecular chaperone CCT2 and CCT5 plays a critical role in stabilizing Cdc20. To explore whether molecular chaperone CCT2 and CCT5 stabilize Cdc20, Vero cells were transfected with CCT2 or CCT5 shRNA for 6 h, followed by transfection with pCI-neo-flag-p10.8 (A) or pCI-neo-flag-σC (B) plasmid DNA for 24 h. Levels of CCT2, CCT5, Cdc20, CDK4, CDK2, and cleaved caspase 3 in pCI-neo-flag-p10.8 or pCI-neo-flag-σC-transfected cells were examined. Signals in all Western blots were quantified with Image J software. The levels of indicated proteins in the mock controls were considered one fold. Protein levels were normalised to those for β-actin. The activation fold indicated below each lane were normalized against values for the mock control.

factors (He et al., 1995; Kitay and Rowe, 1996; Zafrullah et al., 1997; Fournier et al., 1999; Ye et al., 1999; Kornitzer et al., 2001; Poggioli et al., 2001; Heilman et al., 2005; Kim et al., 2008; Huang et al., 2015; Chiu et al., 2016, 2018) or by indirectly elicit cell cycle arrest and apoptosis by disrupting a vital cellular process that causes cell stress (Hoyt et al., 2004; Manju et al., 2006). This study demonstrates that the p10.8 and σC proteins of MDRV facilitate CDK2 and CDK4 degradation via the ubiquitin-proteasome pathway. We demonstrate for the first time that Cdc20 plays a critical role in modulating p10.8- and σC-mediated cell cycle and apoptosis. Furthermore, we demonstrate that molecular chaperone CCT2 and CCT5 are required for stabilization of Ccd20 for mediating both cell cycle arrest and apoptosis. This study provides a novel insight into how p10.8 induces both cell cycle arrest and apoptosis. MDRVs appear to have evolved strategies that alter the physiology of host cells during infection that may benefit virus replication and is related to MDRV-caused necrotic lesions in liver and spleen. Determining how p10.8 and σC proteins modulate host cell cycle progression and apoptosis will enhance understanding of the molecular and cellular basis for MDRV-host interaction and pathogenesis of MDRV. Proposed models illustrating the mechanisms underlying p10.8- and σC-mediated the cell cycle and apoptosis are shown in Figs. 3C and 6 E.

Acknowledgement

This work was supported by grants from The iEGG and Animal Biotechnology Center from The Feature Areas Research Center Program within the framework of the Higher Education Sprout Project by the Ministry of Education (MOE) in Taiwan (108S0023B), the China National Natural Science Foundation (31372474) and the Promote Both Sides of the Taiwan Straits Science and Technology Cooperation Foundation (no. U1305212).

References

Boehme, K.W., Hammer, K., Tollefson, W.C., Konopka-Anstadt, J.L., Kobayashi, T., Dermody, T.S., 2013. Nonstructural protein σ1s mediates reovirus-induced cell cycle arrest and apoptosis. J. Virol. 87, 12967–12979.

Baer, A., Austin, D., Narayanan, A., Popova, T., Kainulainen, M., Bailey, C., Kashanchi, F., Weber, F., Kehn-Hall, K., 2012. Induction of DNA damage signaling upon Rift Valley fever virus infection results in cell cycle arrest and increased viral replication. J. Biol. Chem. 287, 7399–7410.

Boyd, M.T., Vlatkovic, N., Rubbi, C.P., 2011. The nucleolus directly regulates p53 export and degradation. J. Cell Biol. 194 (5), 689–703.

Chaurushiya, M.S., Weitzman, M.D., 2009. Viral manipulation of DNA repair and cell cycle checkpoints. DNA Repair 8, 1166–1176.

Chen, J., Ng, S.M., Chang, C., Zhang, Z., Bourdon, J., Lane, D.P., Peng, J., 2009a. p53 isoform Δ113p53 is a p53 target gene that antagonizes p53 apoptotic activity via BclxL activation in zebrafish. Genes Dev. 23 (3), 278–290.

Chen, S.Y., Chen, S.L., Lin, F.Q., Jiang, B., Wang, S., Cheng, X.X., Zhu, X.L., Zhang, S.Z., Li, Z.L., Cheng, Y.Q., 2009b. The primary study of pathogen of duck hemorrhagic-necrotic hepatitis. Chin. Agric. Sci. Bull. 25, 28–31.

Chen, H., Xu, X., Wang, G., Zhang, B., Wang, G., Xin, G., Liu, J., Jiang, Q., Zhang, H., Zhang, C., 2019. CDK4 protein is degraded by anaphase-promoting complex/ cyclosome in mitosis and reaccumulates in early G_1 phase to initiate a new cell cycle in HeLa cells. J. Biol. Chem. 292 (24), 10131–10141.

Chi, P.I., Huang, W.R., Lai, I.H., Cheng, C.Y., Liu, H.J., 2013. The p17 nonstructural protein of avian reovirus triggers autophagy enhancing virus replication via activation of phosphatase and tensin deleted on chromosome 10 (PTEN) and AMP-activated protein kinase (AMPK), as well as dsRNA-dependent protein kinase (PKR)/eIF2α signaling pathways. J. Biol. Chem. 288 (5), 3571–3584.

Chipuk, J.E., Green, D.R., 2005. Do inducers of apoptosis trigger caspase- independent cell death. Nat. Rev. Mol. Cell Biol. 6, 268–275.

Chiu, H.C., Huang, W.R., Liao, T.L., Wu, H.Y., Munir, M., Shih, W.L., Liu, H.J., 2016. Suppression of vimentin phosphorylation by the avian reovirus p17 through inhibition of CDK1 and Plk1 impacting the G2/M phase of the cell cycle. PLoS One 11 (9), e0162356.

Chiu, H.C., Huang, W.R., Liao, T.L., Chi, P.I., Nielsen, B.L., Liu, J.H., Liu, H.J., 2018. Mechanistic insights into avian reovirus p17-modulated suppression of cell-cycle CDK/cyclin complexes and enhancement of p53 and cyclin H interaction. J. Biol. Chem. 293 (32), 12542–12562.

Chulu, J.L., Lee, L.H., Lee, Y.C., Liao, S.H., Lin, F.L., Shih, W.L., Liu, H.J., 2007. Apoptosis induction by avian reovirus through p53 and mitochondria-mediated pathway. Biochem. Biophys. Res. Commun. 356 (3), 529–535.

Clarke, P., Tyler, K.L., 2003. Reovirus-induced apoptosis: a minireview. Apoptosis 8 (2), 141–150.

Clarke, P., Beckham, J.D., Leser, J.S., Hoyt, C.C., Tyler, K.L., 2009. Fas-mediated apoptotic signaling in the mouse brain following reovirus infection. J. Virol. 83 (12), 6161–6170.

Colón-Ramos, D.A., Irusta, P.M., Gan, E.C., Olson, M.R., Song, J., Morimoto, R.I., Elliott, R.M., Lombard, M., Hollingsworth, R., Hardwick, J.M., Smith, G.K., Kornbluth, S., 2003. Inhibition of translation and induction of apoptosis by Bunyaviral non-structural proteins bearing sequence similarity to reaper. Mol. Biol. Cell 14 (10), 4162–4172.

Costas, C., Martínez-Costas, J., Bodelón, G., Benavente, J., 2005. The second open reading frame of the avian reovirus S1 gene encodes a transcription-dependent and CRM1-independent nucleocytoplasmic shuttling protein. J. Virol. 79, 2141–2150.

De Zio, D., Cianfanelli, V., Cecconi, F., 2013. New insights into the link between DNA damage and apoptosis. Antioxid. Redox. Signal. 19 (6), 559–571.

Fournier, N., Raj, K., Saudan, P., Utzig, S., Sahli, R., Simanis, V., Beard, P., 1999. Expression of human papilloma-virus 16 E2 protein in Schizosaccharomyces pombe

delays the initiation of mitosis. Oncogene 18, 4015–4021.
Frosst, P., Guan, T., Subauste, C., Hahn, K., Gerace, L., 2002. Tpr is localized within the nuclear basket of the pore complex and has a role in nuclear protein export. J. Cell Biol. 156, 617–630.
Funasaka, T., Tsuka, E., Wong, R.W., 2012. Regulation of autophagy by nucleoporin Tpr. Sci. Rep. 2, 878–886.
Geng, H., Zhang, Y., Liu-Partanen, Y., Vanhanseng Guo, D., Wang, Y., Liu, M., Tong, G., 2009. Apoptosis induced by duck reovirus p10.8 protein in primary duck embryonated fibroblast and Vero E6 cells. Avian Dis. 53 (3), 434–440.
Goh, W.C., Rogel, M.E., Kinsey, C.M., Michael, S.F., Fultz, P.N., Nowak, M.A., Hahn, B.H., Emerman, M., 1998. HIV-1 vpr increases viral expression by manipulation of the cell cycle: a mechanism for selection of vpr in vivo. Nat. Med. 4, 65–71.
Guo, D., Qiu, N., Shaozhou, W., Bai, X., He, Y., Zhang, Q., Zhao, J., Liu, M., Zhang, Y., See comment in PubMed Commons below, 2014. Muscovy duck reovirus p10.8 protein localizes to the nucleus via a nonconventional nuclear localization signal. Virol. J. 24 (11), 37.
He, J., Choe, S., Walker, R., Di Marzio, P., Morgan, D.O., Landau, N.R., 1995. Human immunodeficiency virus type 1 viral protein R (Vpr) arrests cells in the G2 phase of the cell cycle by inhibiting p34cdc2 activity. J. Virol. 69, 6705–6711.
Heilman, D.W., Green, M.R., Teodoro, J.G., 2005. The anaphase promoting complex: a critical target for viral proteins and anti-cancer drugs. Cell Cycle 4, 560–563.
Heironymus, D.R., Villegas, K.P., Kleven, S.H., 1983. Identification and serological differentiation of several reovirus strains isolated from chicken with suspected malabsorption syndrome. Avian Dis. 27, 246–254.
Herceg, Z., Wang, Z.Q., 2001. Functions of poly(ADP-ribose) polymerase (PARP) in DNA repair, genomic integrity and cell death. Mutat. Res. 422 (1–2), 97–110.
Hoyt, C.C., Bouchard, R.J., Tyler, K.L., 2004. Novel nuclear herniations nduced by nuclear localization of a viral protein. J. Virol. 78, 6360–6636.
Huang, W.R., Chiu, H.C., Liao, T.L., Chuang, K.P., Shih, W.L., Liu, H.J., 2015. Avian reovirus protein p17 functions as a nucleoporin Tpr suppressor leading to activation of p53, p21 and PTEN and inactivation of PI3K/AKT/mTOR and ERK signaling pathways. PLoS One 10 (8), e0133699.
Kim, S., Park, S.Y., Yong, H., Famulski, J.K., Chae, S., Lee, J.H., Kang, C.M., Saya, H., Chan, G.K., Cho, H., 2008. HBV X protein targets hBubR1, which induces dysregulation of the mitotic checkpoint. Oncogene 27, 3457–3464.
Kitay, M.K., Rowe, D.T., 1996. Cell cycle stage-specific phosphorylation of the Epstein-Barr virus immortal-ization protein EBNA-LP. J. Virol. 70, 7885–7893.
Kominsky, D.J., Bickel, R.J., Tyler, K.L., 2002. Reovirus-induced apoptosis equires both death receptor- and mitochondrial-mediated caspase-dependent pathways of cell death. Cell Death Differ. 9, 926–933.
Kornitzer, D., Sharf, R., Kleinberger, T., 2001. Adenovirus E4orf4 protein induces PP2A-dependent growth arrest in Saccharomyces cerevisiae and interacts with the anaphase-promoting complex/cyclosome. J. Cell Biol. 154, 331–344.
Kroemer, G., Dallaporta, B., Resche-Rigon, M., 1998. The mito-chondrial death/life egulator in apoptosis and necrosis. Annu. Rev. Physiol. 60, 619–642.
Krull, S., Thyberg, J., Bjorkroth, B., Rackwitz, H.R., Cordes, V.C., 2004. Nucleoporins as components of the nuclear pore complex core structure and Tpr as the architectural element of the nuclear basket. Mol. Biol. Cell 15, 4261–4277.
Kuntz-Simon, G., Le Gall-Reculé, G., de Boisséson, C., Jestin, V., 2002. Muscovy duck reovirus sigmaC protein is atypically encoded by the smallest genome segment. J. Gen. Virol. 83, 1189–1200.
Labrada, L., Bodelón, G., Viñuela, J., Benavente, J., 2002. Avian reoviruses cause apoptosis in cultured cells: viral uncoating, but nNot viral gene expression, is required for apoptosis induction. J. Virol. 76 (16), 7932–7941.
Lavoie, J.N., Nguyen, M., Marcellus, R.C., Branton, P.E., Shore, G.C., 1998. E4orf4, a novel adenovirus death factor that induces p53-independent apoptosis by a pathway that is not inhibited by zVAD-fmk. J. Cell Biol. 140, 637–645.
Li, S., Brignole, C., Marcellus, R., Thirlwell, S., Binda, O., McQuoid, M.J., Ashby, D., Chan, H., Zhang, Z., Miron, M.J., Pallas, D.C., Branton, P.E., 2009. The adenovirus E4orf4 protein induces G2/M arrest and cell death by blocking protein phosphatase 2A activity regulated by the B55 subunit. J. Virol. 83 (17), 8340–8352.
Lin, P.Y., Liu, H.J., Lai, M.J., Yu, F.L., Hsu, H.Y., Lee, J.W., Shih, W.L., 2006. Avian reovirus activates a novel proapoptotic signal by linking Src to p53. Apoptosis 11 (12), 2179–2193.
Lin, H.Y., Chuang, S.T., Chen, Y.T., Shih, W.L., Chang, C.D., Liu, H.J., 2007. Avian reovirus-induced apoptosis related to tissue injury. Avian Pathol. 36 (2), 155–159.
Lin, C.H., Shih, W.L., Lin, F.L., Hsieh, Y.C., Kuo, Y.R., Liao, M.H., Liu, H.J., 2009a. Bovine ephemeral fever virus-induced apoptosis requires virus gene expression and activation of Fas and mitochondrial signaling pathway. Apoptosis 14, 864–877.
Lin, P.Y., Lee, J.W., Liao, M.H., Hsu, H.Y., Chiu, S.J., Liu, H.J., Shih, W.L., 2009b. Modulation of p53 by mitogen-activated protein kinase pathways and protein kinase C delta during avian reovirus S1133-induced apoptosis. Virology 385 (2), 323–334.
Lin, P.Y., Liu, H.J., Liao, M.H., Chang, C.D., Chang, C.I., Cheng, H.L., Lee, J.W., Shih, W.L., 2010. Activation of PI 3-kinase/Akt/NF-kappaB and Stat3 signaling by avian reovirus S1133 in the early stages of infection results in an inflammatory response and delayed apoptosis. Virology 400 (1), 104–114.
Lin, P.Y., Liu, H.J., Chang, C.D., Chang, C.I., Hsu, J.L., Liao, M.H., Lee, J.W., Shih, W.L., 2011. Avian reovirus S1133-induced DNA damage signaling and subsequent apoptosis in cultured cells and in chickens. Arch. Virol. 156 (11), 1917–1929.
Lin, P.Y., Liu, H.J., Chang, C.D., Chen, Y.C., Chang, C.I., Shih, W.L., 2015. Avian reovirus S1133-induced apoptosis is associated with Bip/GRP79- mediated Bim translocation to the endoplasmic reticulum. Apoptosis 20 (4), 481–490.
Liu, H.J., Lee, L.H., Hsu, H.W., Kuo, L.C., Liao, M.H., 2003. Molecular evolution of avian reovirus: evidence for genetic diversity and reassortment of the S-class genome segments and multiple cocirculating lineages. Virology 314 (1), 336–349.
Liu, H.J., Lin, P.Y., Lee, J.W., Hsu, H.Y., Shih, W.L., 2005. Retardation of cell growth by avian reovirus p17 through the activation of p53 pathway. Biochem. Biophys. Res. Commun. 336 (2), 709–715.
Liu, H.J., Lin, P.Y., Wang, L.R., Hsu, H.Y., Liao, M.H., Shih, W.L., 2008. Activation of small GTPases RhoA and Rac1 is required for avian reovirus p10-induced syncytium formation. Mol. Cells 26 (4), 396–403.
Los, M., Mozoluk, M., Ferrari, D., Stepczynska, A., Stroh, C., Renz, A., 2002. Activation and caspase-mediated inhibition of PARP: a molecular witch between fibroblast necrosis and apoptosis in death receptor signaling. Mol. Biol. Cell 13, 978–988.
Lozano, G.M., Bejarano, I., Espino, J., González, D., Ortiz, A., García, J.F., Rodríguez, A.B., Pariente, J.A., 2009. Relationship between caspase activity and apoptotic markers in human sperm in response to hydrogem peroxide and progesterone. J. Reprod. Dev. 55 (6), 615–621.
Luo, X., Budihardjo, I., Zuo, H., Slaughter, C., Wang, X., 1998. Bid, a bcl2 interacting protein, mediates cytochrome c release from mitochondria in response to activation of cell surface death receptors. Cell 94, 481–490.
Maclaine, N.J., Hupp, T.R., 2009. The regulation of p53 by phosphorylation: a model for how distinct signals integrate into the p53 pathway. Aging 5, 490–502.
Manju, K., Muralikrishna, B., Parnaik, V.K., 2006. Expression of disease- causing lamin A mutants impairs the formation of DNA repair foci. J. Cell. Sci. 119, 2704–2714.
Marcellus, R.C., Lavoie, J.N., Boivin, D., Shore, G.C., Ketner, G., Branton, P.E., 1998. The early region 4 orf4 protein of human adenovirus type 5 induces p53-independent cell death by apoptosis. J. Virol. 72, 7144–7153.
Murakami, T., Aida, Y., 2014. Visualizing vpr-induced G2 arrest and apoptosis. PLoS One 9 (1), e86840.
O'Donnell, S.M., Hansberger, M.W., Connolly, J.L., Chappell, J.D., Watson, M.J., Pierce, J.M., Wetzel, J.D., Han, W., Barton, E.S., Forrest, J.C., Valyi-Nagy, T., Yull, F.E., Blackwell, T.S., Rottman, J.N., Sherry, B., Dermody, T.S., 2005. Organ-specific roles for transcription factor NF-kappaB in reovirus-induced apoptosis and disease. J. Clin. Invest. 115 (9), 2341–2350.
Orth, J.D., Loewer, A., Lahav, G., Mitchison, T.J., 2012. Prolonged mitotic arrest triggers partial activation of apoptosis, resulting in DNA damage and p53 induction. Mol. Biol. Cell 23 (4), 567–576.
Poggioli, G.J., Dermody, T.S., Tyler, K.L., 2001. Reovirus-induced sigma 1s- dependent G(2)/M phase cell cycle arrest is associated with inhibition of p34(cdc2). J. Virol. 75 (16), 7429–7434.
Pruijssers, A.J., Hengel, H., Abel, T.W., Dermody, T.S., 2013. Apoptosis induction influences reovirus replication and virulence in Newborn Mice. J. Virol. 87 (23), 12980–12989.
Rodriguez-Grille, J., Busch, L.K., Martinez-Costas, J., Benavente, J., 2014. Avian reovirus-triggered apoptosis enhances both virus spread and the processing of the viral nonstructural muNS protein. Virology 462–463, 49–59.
Salsman, J., Top, D., Boutilier, J., Duncan, R., 2005. Extensive syncytium formation mediated by the reovirus FAST proteins ttriggers apoptosis-induced membrane instability. J. Virol. 79 (13), 8090–8100.
Schnitzer, T.J., 1985. Protein coding assignment of the S genes of the avian reovirus S1133. Virology 141 (1), 167–170.
Shieh, S.Y., Ikeda, M., Taya, Y., Prives, C., 1997. DNA damage-induced phosphorylation of p53 alleviates inhibition by MDM2. Cell 91, 325–334.
Shih, W.L., Hsu, H.W., Liao, M.H., Lee, L.H., Liu, H.J., 2004. Avian reovirus sigma C protein induces apoptosis in cultured cells. Virology 321 (1), 65–74.
Shmulevitz, M., Corcoran, J., Salsman, J., Duncan, R., 2004. Cell-cell fusion induced by the avian reovirus membrane fusion protein is regulated by protein degradation. J. Virol. 78 (11), 5996–6004.
Sperka, T., Wang, J., Rudolph, K.L., 2012. DNA damage checkpoints in stem cells, ageing and cancer. Nat. Rev. Mol. Cell Biol. 13, 579–590.
Turnell, A.S., Grand, R.J., 2012. DNA viruses and the cellular DNA-damage response. J. Gen. Virol. 93, 2076–2097.
Vallin, J., Grantham, J., 2019. The role of the molecular chaperone CCT in protein folding and mediation of cytoskeleton-associated processes: implications for cancer cell biology. Cell Stress Chaperones 24, 17–27.
Van der Heide, L., Kalbac, M., Hall, W.C., 1976. Infectious tensynovitis (viral arthritis) influence of maternal antibodies on the development of tensynovitis lesions after experimental infection by day-old chickens with tensynovitis virus. Avian Dis. 20, 641–648.
Wang, Q., Wu, Y., Cai, Y., Zhuang, Y., Xu, L., Wu, B., Zhang, Y., 2015a. Spleen transcriptome profile of muscovy ducklings in response to infection with muscovy duck reovirus. Avian Dis. 59 (2), 282–290.
Wang, J.Y., Chen, Z.L., Li, C.S., Cao, X.L., Wang, R., Tang, C., Huang, J.J., Chang, C.D., Liu, H.J., 2015b. The distribution of sialic acid receptors of avian influenza virus in the reproductive tract of laying hens. Mole. Cell Probes 29 (2), 129–134.
Wang, Q., Liu, M., Xu, L., Wu, Y., Huang, Y., 2018a. Transcriptome analysis reveals the molecular mechanism of hepatic fat metabolism disorder caused by Muscovy duck reovirus infection. Avian Pathol. 47 (2), 127–139.
Wang, Q., Yuan, X., Chen, Y., Zheng, Q., Xu, L., Wu, Y., 2018b. Endoplasmic reticulum stress mediated MDRV p10.8 protein-induced cell cycle arrest and apoptosis through the PERK/eIF2α pathway. Front. Microbiol. 9, 1327.
Wang, Q., Liu, M., Chen, Y., Xu, L., Wu, B., Wu, Y., Huang, Y., Huang, W.R., Liu, H.J., 2019. Muscovy duck reovirus p10.8 protein induces ER stress and apoptosis through the Bip/IRE1/XBP1 pathway. Vet. Microbiol. 228, 234–245.
Weinstein, J., Jacobsen, F.W., Hsu-Chen, J., Wu, T., Baum, L.G., 1994. A novel mammalian protein, p55CDC, present in dividing cells is associated with protein kinase activity and has homology to the Saccharomyces cerevisiae cell division cycle proteins Cdc20 and Cdc4. Mol. Cell. Biol. 14 (5), 3350–3363.
Weinstein, J., 1997. Cell cycle-regulated expression, phosphorylation, and degradation of p55Cdc. A mammalian homolog of CDC20/Fizzy/slp1. J. Biol. Chem. 272 (45), 28501–28511.

Wu, B.C., Chen, J.X., Yao, J.S., 2001. Isolation and identification of muscovy duck reovirus. J. Fujian Agricult. Forestry Univ. (Natural Science Edition, in Chinese) 3 (2), 227–230.
Wu, Y., Cui, L., Zhu, E., Zhou, W., Wang, Q., Wu, X., Wu, B., Huang, Y., Liu, H.J., 2017. Muscovy duck reovirus σNS protein triggers autophagy enhancing virus replication. Virol. J. 14 (1), 53.
Ye, M., Duus, K.M., Peng, J., Price, D.H., Grose, C., 1999. Varicella-zoster virus Fc receptor component gI is phosphorylated on its endodomain by a cyclin-dependent kinase. J. Virol. 73, 1320–1330.
Yuan, Y.H., Wang, J.F., Wu, Z.X., Huang, X.G., He, D.S., Huang, S.J., 2013. Biological identification of a new-type duck reovirus (QY strains) isolated from Muscovy duck. Chin. J. Vet. Sci. 33, 40–44.
Yun, T., Yu, B., Ni, Z., Ye, W., Chen, L., Hua, J., Zhang, C., 2014. Genomic characteristics of a novel reovirus from Muscovy duckling in China. Vet. Microbiol. 168 (2-4), 261–271.
Zafrullah, M., Ozdener, M.H., Panda, S.K., Jameel, S., 1997. The ORF3 protein of hepatitis E virus is a phosphoprotein that associates with the cytoskeleton. J. Virol. 71, 9045–9053.
Zamarin, D., Garcia-Sastre, A., Xiao, X., Wang, R., Palese, P., 2005. Influenza virus PB1-F2 protein induces cell death through mitochondrial ANT3 and VDAC1. PLoS Pathog. 1, e4.
Zhao, R.Y., Elder, R.T., 2005. Viral infections and cell cycle G2/M regulation. Cell Res. 15 (3), 143–149.